

Link to publisher version: <https://doi.org/10.1016/j.fuel.2022.125030>

Partial hydrogenation of FAMEs with high content of C18:2 dienes.
Selective hydrogenation of tobacco seed oil-derived biodiesel

Eugenio Quaranta^{a,b,*}, Angela Dibenedetto^{a,b}, Antonella Colucci^b, Daniele Cornacchia^{a,b}

^a*Università degli Studi di Bari “Aldo Moro”, Dipartimento di Chimica, via E. Orabona, 4, 70126*

Bari, Italy

^b*Consorzio Interuniversitario “Reattività Chimica e Catalisi”, via Celso Ulpiani, 27, 70126 Bari,*

Italy

* Corresponding author. *E-mail address:* eugenio.quaranta@uniba.it

ABSTRACT

The study reports on Pd(5%)/C-catalyzed partial hydrogenation of two C18:2-rich FAME mixtures (66.9 and 75.1 mol% C18:2) respectively prepared by esterification of technical linoleic acid and transesterification of tobacco seed oil. The mixtures were taken as representatives of C18:2-rich FAMEs obtainable from a variety of non-edible oils, which have potential as alternative feedstocks for the development of 2nd-generation biodiesel. In *n*-heptane, under mild conditions (15 °C; 0.1 MPa H₂; 45-60 min; Pd/C, 2.1-5.7 wt%), the FAME mixtures were converted to C18:1 with high yield (83-92%) and selectivity (93-95%). Stearate abundance in the hydrogenated mixture was kept in acceptable limits (5.5-8.1%); *E*-C18:1 formation and C=C scattering were respectively in the ranges 20.3-34.8% and 15-24%. At 0 °C, under moderate H₂ pressure (1 MPa), the formation of *trans*-C18:1 monoenes and C=C scrambling were less pronounced and respectively equal to 9.0% and 7% after 45 min, using a lower catalyst load (1.0 wt%): under the latter conditions the C18:2-component was markedly curtailed (66.9→13.6%) in the final product, while stearate abundance was still quite modest (9.3%). Geometric and positional isomerization increased over time with the progress of C18:2 conversion and were favored by higher temperature and catalyst load. Under

25 solventless conditions hydrogenation was slower than in *n*-heptane; moreover, both *cis*→*trans*
26 isomerization and C=C bond scattering were larger than in the hydrocarbon solvent. Remarkably,
27 Pd/C can act as a versatile catalyst, being able to effectively promote the conversion of the FAME
28 mixtures to stearate under uncommon very mild conditions.

29

30 *Keywords:* FAMEs partial hydrogenation; methyl stearate; Pd/C; second-generation biodiesel;
31 tobacco seed oil

32

33 1. Introduction

34 Over the last few years selective partial hydrogenation of poly-unsaturated FAMES (Fatty
35 Acid Methyl Esters) to mono-unsaturated methyl esters has been arousing lively interest as
36 attractive gateway to upgraded biodiesel [1-3]. FAMES, mostly obtained by methanolysis of
37 triglyceride mixtures extracted from renewable resources such as vegetable oils [4-7], fish oils [7,8],
38 animal fats [7], waste frying oils [7,9], are basic components of biodiesel, whose characteristics
39 depend critically on the fatty acid profile of feedstock used in the transesterification step. In fact,
40 structural features such as FAMES chain length and unsaturation degree markedly affect several
41 biodiesel properties such as cetane number, heat of combustion, viscosity, oxidation stability,
42 surface tension, lubricity [5]. Partial hydrogenation, by lowering the content of polyenes in the
43 FAME raw mixture, can modify and upgrade biodiesel properties significantly. For instance,
44 reducing the level of FAMES with a degree of unsaturation higher than 1 can markedly improve
45 biodiesel stability to oxidation. However, the content of fully saturated FAMES, as well as the
46 extent of both *cis*→*trans* and positional isomerization, must be carefully controlled throughout the
47 hydrogenation process and kept as low as possible in the hydrogenated mixture in order to preserve
48 the cold flow properties of final product. Controlling both selectivity to monoene and incidence of
49 isomerization (geometrical and positional) side-processes is a major issue that makes partial
50 hydrogenation of poly-unsaturated FAMES a challenging task.

51 Commonly explored feedstocks for biodiesel production are vegetal oils, often relevant to
52 food chain, whose fatty acid profile shows relatively low to moderate (max. ~50%) content of
53 C18:2 dienes in addition to variable amounts of other components (mostly C18:1) [6,7].
54 Accordingly, a lot of studies have been addressed to improve the oxidative stability of FAME
55 mixtures obtained from rapeseed oil [10,11], canola oil [12], soybean oil [13,14], jatropha oil [15],
56 palm oil [16] corn oil [17] by partial hydrogenation of C18:m polyenes to C18:1 methyl esters [2,3].
57 Several studies in this area have considered supported metal catalysts and focused on the catalyst

58 type [10,18], catalyst preparation and support properties [19-22], reaction conditions and type of
59 reactor [23]. In comparison, partial hydrogenation of FAMEs with a higher content of C18:2 has
60 received much less attention. A few studies have focused on the selective hydrogenation of FAMEs
61 derived from edible high-linoleic sunflower oil (~65 mol% C18:2) and explored the activity of a
62 variety of catalytic systems such as transition M-complexes (M = Ni, Ru, Pd, Rh) [24-29], Pd
63 nanoparticles in polyethylene glycol [30] or ionic liquids [31], heterogeneous Pd catalysts supported
64 on carbon-coated monoliths [32-34]. To date, partial hydrogenation of FAMEs with an even higher
65 C18:2 content (> 70 mol%) has been matter of very few sporadic studies [35,36] involving grape-
66 seed oil-, safflower oil-, tobacco seed oil-derived FAMEs, that have been partially hydrogenated
67 over Cu-supported heterogeneous catalysts [35-37].

68 However, partial hydrogenation of C18:2-rich FAMEs deserves greater attention.
69 Nowadays, economic, ethical and social reasons urge to replace edible by non-edible oils for
70 biodiesel production and to search lower-cost reliable feedstocks, included those that have already
71 fulfilled their food purpose (waste oily streams from the oil refinery, waste cooking oils, waste
72 animal fats) [7,9,38-40]. Noteworthy, several C18:2-rich FAME mixtures can be obtained from
73 non-edible oils derived from non-food low-cost crops (*Argemone mexicana*, *Melia azadirach* Linn.,
74 *Melia azedarach*, *Papaverum Somniferum* L., *Idesia polycarpa* var. *vestita*, *Nicotiana tabacum* L.,
75 etc.) and may play an important role in the development of 2nd-generation biodiesel. Herein, we
76 focus on partial hydrogenation of two C18:2-rich FAME mixtures (C18:2 > 65 mol%) selected as
77 case studies. The study includes a rare example of selective partial hydrogenation of biodiesel (~75
78 mol% C18:2) derived from tobacco seed oil (TSO). In the last few years, TSO has been regarded as
79 a new feedstock for biodiesel production [41-43]. Tobacco is a plant well-known for the leaves used
80 to manufacture cigarettes and cigars, but it also produces huge amount of small seeds that,
81 generally, are not collected as they do not display any commercial value. However, tobacco seed
82 has potential to become a commercial product as it contains significant amounts of non-edible oil
83 (35–49 wt%) that has been proposed for biodiesel production. Most of properties of TSO-derived

84 biodiesel meet the specifications of the European Biodiesel Standard EN14214 except oxidation
85 stability and iodine value because of high C18:2 FAME content. To circumvent this drawback, the
86 addition of antioxidants (tert-butylhydroquinone, propyl gallate, pyrogallol, butylated anisole, etc)
87 has been explored [43]. However, the use of additives often puts additional problems as, in
88 principle, these substances need to be compatible with biodiesel and should not affect other fuel
89 properties negatively. In this ambit, therefore, selective partial hydrogenation of biodiesel may
90 provide a suitable alternative approach to face this issue.

91 In the present study a reliable commercial Pd/C (Pd on carbon) catalyst has been selected to
92 promote the hydrogenation process. Pd is as a very promising metal for partial hydrogenation of
93 polyunsaturated FAMES [2,3] and Pd/C, in particular, offers a few practical advantages (low cost
94 and availability of support, easy metal recovery) [44]. Pd/C catalysts have been successfully used in
95 upgrading fish oil-derived biodiesel ~20% rich in polyenes (≥ 4 double bonds) [8] and in the partial
96 hydrogenation of C18:3-rich (~75%) FAMES [45]. This choice provided a sound starting point to
97 explore the spectrum of transformations occurring in the selective hydrogenation of FAMES with a
98 so high C18:2 content. The influence of a few experimental parameters (temperature, time, H₂
99 pressure, catalyst load) on key features of the process such as C18:1 yield, monoene-selectivity,
100 formation of *cis/trans* and positional isomers has been investigated with the target of conjugating
101 high C18:m (m = 2,3) conversion with good C18:1-, regio- and stereo-selectivity. The results have
102 been compared with those available in the literature for partial hydrogenation of FAME mixtures of
103 comparable composition in presence of other catalytic systems.

104 **2. Materials and methods**

105 *2.1. General*

106 Manipulations performed under an inert atmosphere (N₂) were carried out by using vacuum
107 line techniques. The FAME mixtures considered in this study, hereafter named “mixture A” and
108 “mixture B”, were respectively obtained *a*) by esterification of a commercial mixture (Linoleic acid

109 technical, 60-74%, Sigma-Aldrich) of (9Z,12Z)-octadeca-9,12-dienoic acid (linoleic acid) and (9Z)-
110 octadec-9-enoic acid (oleic acid) and *b*) by transesterification of tobacco seed oil with
111 methanol/KOH. The FAME mixtures, once isolated, were stored at -20 °C and manipulated under
112 N₂. Their composition is reported in Tables S1-S4 (entry 1). Diethyl ether, MeOH, *n*-hexane
113 (Sigma-Aldrich, ACS grade) and *n*-heptane (Carlo Erba, RPE) were used as received. H₂
114 (99.9999% purity) was generated electrolytically by means of a H₂ generator (DBS Mod. NMH₂-
115 250). The catalyst, Pd(5%)/C, was a commercial product (Lancaster Synthesis). It was dried under
116 vacuum for 1 h at 150 °C before use. GC analyses were carried out with a TRACE™ 1310 GC
117 equipped with a flame ionization detector and a BPX-70 capillary column (70% cyanopropyl
118 polysilphenylene-siloxane; 120 m, i.d. 0.25 mm, film thickness 0.20 μm): detector/injector, 250
119 °C/225 °C; oven, 100 °C/10 °Cmin⁻¹/140 °C/5 °Cmin⁻¹/165 °C (20 min)/1 °Cmin⁻¹/170 °C (10
120 min)/1 °Cmin⁻¹/180 °C (10 min)/10 °Cmin⁻¹/220 °C (10 min); injected volume, 1 μL; split ratio,
121 100/1; carrier, He (1 mL/min). The fatty acid methyl esters were identified by their elution times
122 with known standards. Typical standard error was within ±3%. NMR spectra were recorded with a
123 Varian Inova 400 spectrometer. Chemical shifts are in δ(ppm) vs TMS (tetramethylsilane).

124 Throughout the text the locutions “monoene (or C18:1) component”, “diene (or C18:2)
125 component” and “triene (or C18:3) component” refer, respectively, to the total amount of *cis/trans*
126 mono-unsaturated, *cis/trans* di-unsaturated and *cis/trans* tri-unsaturated FAMEs present in the
127 reaction mixture, irrespective of C=C double bond position. In the case of the FAME mixture B,
128 that contained also minor amounts of C18:3 trienes (<1 mol%), the conversion of the starting
129 C18:*m* (*m* = 2, 3) mixture (C_{C18:*m*}), the yield of C18:1 FAMEs (Y_{C18:1}), and the selectivity to C18:1
130 monoenes (S_{C18:1}) were respectively calculated by means of Equations (1a)-(3a), where $mol^{\circ}_{C18:m}$
131 (*m* = 2, 3) are the initial moles of the C18:*m* (*m* = 2, 3) component, $mol_{C18:m,consumed}$ are the

132 consumed moles of C18:m (m = 2, 3) polyenes, and $\Delta mol_{C18:m}$ is the molar increment ($\Delta mol_{C18:m} \geq$
 133 0) of the C18:m (m = 0, 1, 2) component relative to the initial value.¹

$$134 \quad C_{C18:m(m=2,3)} = \frac{mol_{C18:3,consumed} + mol_{C18:2,consumed}}{mol^o_{C18:3} + mol^o_{C18:2}} \times 100 \quad (1a)$$

$$135 \quad Y_{C18:1} = \frac{\Delta mol_{C18:1}}{mol^o_{C18:3} + mol^o_{C18:2}} \times 100 \quad (2a)$$

$$136 \quad S_{C18:1} = \frac{\Delta mol_{C18:1}}{\Delta mol_{C18:2} + \Delta mol_{C18:1} + \Delta mol_{C18:0}} \times 100 \quad (3a)$$

137 In the case of the FAME mixture A, that did not contain C18:3 trienes, the Equations (1a)-
 138 (3a) convert into the simpler Equations (1b)-(3b).¹

$$139 \quad C_{C18:2} = \frac{mol_{C18:2,consumed}}{mol^o_{C18:2}} \times 100 \quad (1b)$$

$$140 \quad Y_{C18:1} = \frac{\Delta mol_{C18:1}}{mol^o_{C18:2}} \times 100 \quad (2b)$$

$$141 \quad S_{C18:1} = \frac{\Delta mol_{C18:1}}{\Delta mol_{C18:1} + \Delta mol_{C18:0}} \times 100 \quad (3b)$$

142 The selectivity to *cis*-C18:1 monoenes ($S_{cis-C18:1}$) has been expressed as the ratio between the
 143 moles of *cis*-C18:1 monoenes produced, $\Delta mol_{cis-C18:1}$ ($\Delta mol_{cis-C18:1} \geq 0$), and the overall moles of
 144 C18:1 monoenes obtained, $\Delta mol_{C18:1}$ (Equation (4)). Likewise, the selectivity to C18:1(n-x)
 145 monoenes (x = 9 or 6), $S_{C18:1(n-x)}$, was given by the ratio of the moles of C18:1(n-x) monoenes
 146 formed, $\Delta mol_{C18:1(n-x)}$ ($\Delta mol_{C18:1(n-x)} \geq 0$), over the total moles of C18:1 monoenes produced,
 147 $\Delta mol_{C18:1}$ (Equations (5) and (6)).^{2,3}

$$148 \quad S_{cis-C18:1} = \frac{\Delta mol_{cis-C18:1}}{\Delta mol_{C18:1}} \times 100 \quad (4)$$

$$149 \quad S_{C18:1(n-9)} = \frac{\Delta mol_{C18:1(n-9)}}{\Delta mol_{C18:1}} \times 100 \quad (5)$$

¹ $\Delta mol_{C18:m}$ was placed equal to zero when the abundance of the relevant C18:m component in the hydrogenated mixture was lower than the starting value. Consequently, $Y_{C18:1}$ or $S_{C18:1}$ were equal to zero whenever C18:1 abundance in the final product was found to be lower than the initial value ($\Delta mol_{C18:1} < 0$), in accordance with the fact that, in these cases, there was not net formation of C18:1 monoenes.

² $\Delta mol_{cis-C18:1}$ and $\Delta mol_{C18:1(n-9)}$ were respectively placed equal to zero when the abundances of the relevant components (*cis*-C18:1 and C18:1(n-9)) in the hydrogenated mixture were lower than the initial value ($\Delta mol < 0$). Consequently, in these cases, also $S_{cis-C18:1}$ and $S_{C18:1(n-9)}$ were equal to zero, in accordance with the fact that there was no net production of *cis*-C18:1 or C18:1(n-9) monoenes.

³ The calculation of $S_{cis-C18:1}$ or $S_{C18:1(n-x)}$ (x = 6, 9) was meaningless when no net formation of C18:1 monoenes ($\Delta mol_{C18:1} \leq 0$) was found in the final product.

$$S_{C_{18:1}(n-6)} = \frac{\Delta mol_{C_{18:1}(n-6)}}{\Delta mol_{C_{18:1}}} \times 100 \quad (6)$$

151 $S_{cis-C_{18:1}}$ measures the distribution of *cis/trans* stereoisomers in the C18:1 component. $S_{C_{18:1}(n-9)}$ and
 152 $S_{C_{18:1}(n-6)}$ provide a useful tool for comparing, respectively, the formation of the positional isomers
 153 C18:1(n-9) and C18:1(n-6).⁴

154

155 2.2. Preparation of FAME mixture A

156 In a 500 mL flask a methanol (140 mL) solution containing 1.8 mL of concentrated H₂SO₄
 157 was added to technical linoleic acid (90.2 g, 100 mL). The reaction mixture was refluxed for 6 h
 158 and then cooled to room temperature. Methanol was removed by evaporation under vacuum and the
 159 residue was treated with diethyl ether. The ethereal solution was washed with aqueous NaCl
 160 (3×100 mL), aqueous KHCO₃ (1×150 mL), then it was dried over anhydrous MgSO₄, filtered and
 161 evaporated under vacuum. The resulting FAME mixture (100 mL) was finally analyzed by GC.

162 2.3. Oil extraction from tobacco seeds

163 Tobacco seeds (*Nicotiana tabacum* L.) were produced in fields located in Campania (Italy).
 164 The seeds were dried using a moisture analyzer (KERN MRS 120-3) at 80 °C until no weight
 165 reduction was registered, then they were ground by means of a planetary ball mill “Fritsch
 166 Pulverisette 7” for 30 min at 700 rpm and treated with liquid nitrogen (15 mL/g_{biomass}) to break the
 167 cell membrane. The ground seeds (10 g) and *n*-hexane (100 mL) were introduced into a Soxhlet
 168 apparatus and the mixture was refluxed for 8 h. The extracted liquid was transferred to a rotary
 169 vacuum evaporator and the solvent was removed under vacuum at the temperature of 65 °C. Oil

⁴ The sum $S_{C_{18:1}(n-9)} + S_{C_{18:1}(n-6)} (\leq 100)$ correlates roughly with the extent of C=C bond scrambling in the C18:1 component, that can be estimated as follows:

$$[(\%)C_{18:1}(\text{total}) - (\%)C_{18:1}(n-9) - (\%)C_{18:1}(n-6)] \times 100 / (\%)C_{18:1}(\text{total}).$$

(%)C_{18:1}(total) is the overall abundance of C18:1 monoenes and (%)C_{18:1}(n-x) (x = 6, 9) is the abundance of the C18:1(n-x) (x = 6, 9) component. The C18:1(n-x) (x = 6, 9) abundances can be calculated from the data in the Tables S1- S4 as follows:

$$(\%)C_{18:1}(n-9) = (\%)E-C_{18:1}(n-9) + (\%)Z-C_{18:1}(n-9);$$

$$(\%)C_{18:1}(n-6) = (\%)E-C_{18:1}(n-6) + (\%)Z-C_{18:1}(n-6).$$

170 yield: 41% (w/w) on dry basis. Oil characterization (see ref. [46]): free fatty acid, 1.1%;
171 unsaponifiable matter, 1.1%; monoglycerides, <0.1%; diglycerides, 1.7%; triglycerides, 96.6%.

172 2.4. Preparation of METSO mixture B

173 A methanol (60 mL) solution, containing 7.8 g of KOH previously solubilized in 3 mL of
174 H₂O, was added to 11.08 g of TSO dissolved in 120 mL of *n*-hexane. The mixture was vigorously
175 stirred for 20 min at room temperature. The hexane phase was recovered and the remaining mixture
176 was further extracted with more *n*-hexane (2×100 mL). The hexane fractions were collected and
177 washed with H₂O (3×50 mL). The organic phase was dried over anhydrous MgSO₄, filtered and
178 evaporated under vacuum. The resulting METSO mixture (10.31 g) was finally analyzed by GC.

179 2.5. Catalytic hydrogenation of the FAME mixtures: general procedure

180 Into a Schlenck tube, equipped with a screw cap and a torion stopcock, the catalyst (19-52
181 mg), the FAME mixture (1 mL) and *n*-heptane (5 mL) were introduced under a dinitrogen stream.
182 The mixture was frozen using a cold bath and, after removing N₂ under vacuum, was heated to the
183 working temperature (0-40 °C). The reactor was then connected to a gas bag filled with H₂ (excess)
184 at atmospheric pressure (0.1 MPa). The suspension was stirred (350 rpm) for a pre-set time at the
185 working temperature and, then, filtered. The liquid phase, suitably diluted to a final volume of 100
186 mL with more *n*-heptane, was analyzed by GC using methyl heptadecanoate C17:0 (50-100 µL) as
187 internal standard.

188 The experiments under H₂ pressure were carried out in a steel autoclave (inner volume, 50
189 mL). Typically, a cylindric glass reactor charged under a dinitrogen stream with FAME mixture A
190 (1 mL), the catalyst (9-51 mg) and *n*-heptane (5 mL), if used, was introduced into the autoclave
191 previously purged with N₂. The autoclave was sealed, cooled to 0 °C, and loaded with H₂ (1 MPa).
192 The system was allowed to react at 0 °C for a pre-set time (stirring rate: 350 rpm). The reaction

193 solution was then filtered to remove the catalyst, diluted to 100 mL with more *n*-heptane and
 194 analyzed by GC.

195 3. Results

196 3.1. Partial hydrogenation of FAME mixture A

197 Under non severe conditions (0-40 °C, 0.1 MPa H₂) FAME mixture A (see 2.2) can be easily
 198 hydrogenated over Pd/C (5.7 wt%) in *n*-heptane as reaction medium (Tables 1 and S1).

199 At 0 °C (Fig. S1), the hydrogenation process was initially (≤60 min) very selective
 200 (>95%), but both C18:2 conversion (C_{C18:2}) and C18:1 yield (Y_{C18:1}) were still moderate
 201 (respectively 67.0% and 64.4%, after 1 h; Table 1, entry 5). For longer reaction times S_{C18:1} and
 202 Y_{C18:1} decreased dramatically because of heavy formation of stearate.

203 At moderately higher temperatures (≥30 °C) the hydrogenation reaction was faster, but the
 204 control of selectivity was more difficult. After 1 h at 30 °C, C_{C18:2} was practically quantitative
 205 (99.7%; entry 8, Table 1), but C18:1 monoenes in the final mixture did not exceed 8%, showing that
 206

Table 1

Partial hydrogenation (0.1 MPa H₂) of FAME mixture A (1 mL) over Pd/C (catalyst load: 5.7 wt%) in *n*-heptane (5 mL): influence of temperature and reaction time on yield and selectivities.

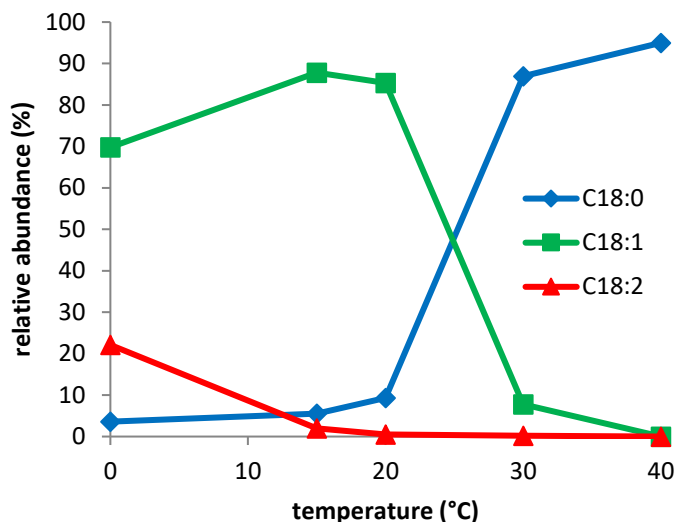
Entry	T (°C)	t (min)	C _{C18:2}	Y _{C18:1}	S _{C18:1}	S _{cis-C18:1}	S _{C18:1(n-9)}	S _{C18:1(n-6)}	S _{C18:1(n-9)+S_{C18:1(n-6)}}
1	0	30	44.7	43.6	97.3	71.6	41.8	40.4	82.2
2	15	30	69.4	65.6	96.7	48.3	36.0	30.3	66.3
3	30	30	98.9	90.3	91.8	29.0	31.4	29.0	60.4
4	40	30	98.5	35.7	36.2	0 ^a	0 ^a	31.4	31.4
5	0	60	67.0	64.4	95.8	60.8	39.2	36.7	75.9
6	15	60	97.0	91.3	94.1	43.0	35.0	31.4	66.4
7	20	60	99.2	87.6	88.5	b	b	b	b
8	30	60	99.7	0 ^c	0 ^c	d	d	d	d
9	40	60	100	0 ^c	0 ^c	d	d	d	d

^a See footnote [2] in the main text and Table S1 (entry 11).

^b Not determined.

^c See footnote [1] in the main text and the relevant entry in Table S1.

^d See footnote [3] in the main text and the relevant entry in Table S1.



208

209 **Fig. 1.** Partial hydrogenation (0.1 MPa H₂) of FAME mixture A (1 mL) over Pd/C (catalyst load:
210 5.7 wt%) in *n*-heptane (5 mL) after 1 h at different temperatures.

211

212 most of the C18:1 component initially present in the FAME mixture was converted to C18:0 (Fig.
213 1; entry 10, Table S1); after 1 h at 40 °C the C18:1 component vanished at all, and stearate formed
214 selectively (100%) in quantitative yield (Fig. 1; entry 12, Table S1). Shorter reaction times allowed
215 a relatively better control of the hydrogenation process. Accordingly, at 30 °C, C18:1 yield and
216 selectivity respectively as high as 90.3% and 91.8% were achieved by halving the reaction time (30
217 min; entry 3, Table 1). However, under the latter conditions, while double bond scrambling was still
218 moderate (as it can be deduced from the sum $S_{C18:1(n-9)}+S_{C18:1(n-6)}$ equal to 60.4%), the formation of
219 *E*-C18:1 monoenes was large, as supported by the value of $S_{cis-C18:1}$ (29.0%).

220 The above data emphasize the key role of temperature and reaction time in controlling yield
221 and selectivity of the process. Accordingly, appreciably better results were obtained by reacting the
222 system at 15 °C for 1 h (Entry 6, Table 1; Entry 7, Table S1). Under the above conditions $C_{C18:2}$
223 (97.0%) was slightly lower than at 30°C after 30 min (98.9%; Entry 3, Table 1), but both yield and
224 selectivities were more attractive, as it can be inferred from the values of $Y_{C18:1}$, $S_{C18:1}$, $S_{cis-C18:1}$,
225 $S_{C18:1(n-9)}$, $S_{C18:1(n-6)}$ and the sum $S_{C18:1(n-9)}+S_{C18:1(n-6)}$ (compare entries 6 and 3 in Table 1).

226 The resulting hydrogenated mixture was analyzed by NMR. The proton spectrum of the
227 reaction mixture at the end of the catalytic run confirmed the quantitative conversion of linoleate, as

228 supported by the disappearance of the triplet **A** due to the methylene protons H11_{linoleate} (Fig. S2).
 229 Accordingly, in the ¹³C spectrum of the hydrogenated mixture (Fig. S3) the resonance **F** of
 230 C11_{linoleate} was no longer evident, as well as the signals **B** at 130.17, 130.00, 128.02 and 127.88
 231 ppm, respectively due to the linoleate carbons C13, C9, C10 and C12. The ¹³C spectrum of the
 232 hydrogenated mixture showed, besides the oleate resonances **C** at 129.66 and 129.90 ppm (C9 and
 233 C10), also several new resonances in the region 129.7-130.5 ppm assigned to new mono-
 234 unsaturated isomeric species. The appearance of these resonances was accompanied by that of new
 235 signals **D** around 27.2 ppm, where the resonances of the allylic carbons in *cis*-C18:1 monoenes are
 236 usually located, and **E**, close to 32.5 ppm, assigned to allylic carbons in *trans*-C18:1 monoenes.
 237 Overall, the NMR results agree with the fact that oleate formation is accompanied by the generation
 238 of *cis*-C18:1 and *trans*-C18:1 positional isomers.

239 The process was also investigated under pressure of H₂ (1 MPa) at a temperature as low as 0
 240 °C that, as documented in the experiments carried out at atmospheric pressure (see Fig. S1), allows
 241 an easier control of selectivities ($S_{C18:1}$, $S_{cis-C18:1}$, $S_{C18:1(n-9)}$ and $S_{C18:1(n-6)}$), at least for relatively short
 242 reaction times. The results of this study are summarized in Table 2 and Table S2. Under pressure of
 243 H₂, C18:2 conversion to C18:1 was much faster but less selective (compare, for instance, entries 1
 244 and 2 in Table 2). With a catalyst load of 2.1 wt% C_{C18:2} was almost complete (99.2%) after 20 min,
 245 while $S_{C18:1}$ and $S_{cis-C18:1}$ were close to 74% and 61%, respectively (entry 3, Table 2). Further

Table 2

Partial hydrogenation (1 MPa H₂, 0 °C) of FAME mixture A (1 mL) over Pd/C in *n*-heptane (5 mL).

Entry	catalyst load (wt%)	t (min)	C _{C18:2}	Y _{C18:1}	S _{C18:1}	S _{<i>cis</i>-C18:1}	S _{C18:1(n-9)}	S _{C18:1(n-6)}	S _{C18:1(n-9)} +S _{C18:1(n-6)}
1 ^a	5.7	30	46.3	43.6	93.9	71.6	41.8	40.4	82.2
2	5.7	30	100	65.2	66.7	44.3	34.8	45.9	80.7
3	2.1	20	99.2	73.5	74.1	60.7	39.0	46.3	85.3
4	1.0	30	66.2	56.8	86.2	80.8	44.7	45.8	90.5
5	1.0	45	79.7	67.7	85.6	80.1	44.1	46.3	90.4
6	1.0	60	100	43.5	43.6	0 ^b	16.1	50.5	66.6

^a Under 0.1 MPa of H₂.

^b See footnote [2] in the main text and Table S2 (entry 6).

246 diminution of catalyst load slowed down the process but allowed to better control the hydrogenation
247 of the diene component. Using a catalyst load as low as 1.0 wt%, the conversion was close to 80%
248 after 45 min (entry 5, Table 2; see also Fig. S4). Under the latter conditions, the yield ($Y_{C18:1}$) was a
249 bit less satisfactory (67.7 vs 73.5%; entry 3, Table 2), but both $S_{C18:1}$ and $S_{cis-C18:1}$ were higher
250 (85.6% and 80.1%, respectively), while the sum $S_{C18:1(n-9)}+S_{C18:1(n-6)}$ was close to 90%.

251 3.2. *Partial hydrogenation of METSO mixture B*

252 The study has been extended to the C18:2 richer METSO mixture B (see 2.4). The
253 hydrogenation was studied at atmospheric pressure of H_2 , at the temperature of 15 °C (Tables 3 and
254 S3), under conditions that, when applied to mixture A (see 3.1), led to a better compromise between
255 polyene conversion and C18:1 yield and selectivity.

256 Using a catalyst load close to 6 wt% (entries 4-6, Table 3; Fig. S5), the conversion of the
257 starting diene was complete within 45 min. However, $S_{C18:1}$, that was very high (95.4%) after 30
258 min, decreased fast to 72.4% after 45 min because of large stearate formation (23.4%; Fig. S5a).

259 Much more satisfactory results were obtained by lowering the catalyst load as illustrated in
260 Fig. 2 that displays the results obtained after a reaction time of 45 min when varying the catalyst
261 load in the range 8.2-2.1 wt%. The use of a higher catalyst load (8.2 wt%) sped up the conversion to
262 stearate (Fig. 2a) to detriment of C18:1 yield (42.3%) and selectivity (42.9%) (Fig. 2c). After 1 h
263 under the above conditions stearate formed with 93.3% yield (Entry 9, Table S3). Practically
264 quantitative linoleate conversion (98.9%) with high C18:1 yield (91.7%) and selectivity (92.8%)
265 was achieved with a catalyst load of 3.4 wt% (Fig. 2c). The use of a catalyst load as low as 2.1 wt%
266 led to a lower yield (83.3%) but increased both $S_{C18:1}$ (94.9%) and $S_{cis-C18:1}$ (67.9%) (Fig. 2c). Under
267 the latter conditions (Entry 1, Table 3) also double bond scrambling was more moderate, as
268 suggested by the value of the sum $S_{C18:1(n-9)}+S_{C18:1(n-6)}$ that was equal to 83%.

269

Table 3

Partial hydrogenation (0.1 MPa H₂, 15°C) of METSO mixture B (1 mL) over Pd/C in *n*-heptane (5 mL): influence of catalyst load and reaction time on yield and selectivities.

Entry	Catalyst load (wt%)	t (min)	C _{C18:m (m = 2,3)}	Y _{C18:1}	S _{C18:1}	S _{cis-C18:1}	S _{C18:1(n-9)}	S _{C18:1(n-6)}	S _{C18:1(n-9)+S_{C18:1(n-6)}}
1	2.1	45	87.5	83.3	94.9	67.9	42.2	40.8	83.0
2	3.4	45	98.9	91.7	92.8	52.9	39.5	36.8	76.3
3	3.4	60	99.3	60.6	61.6	7.6	5.0	29.3	34.3
4	5.7	30	75.8	72.2	95.4	58.0	31.0	34.3	65.3
5	6.1	45	99.6	71.5	72.4	a	a	a	a
6	5.6	60	99.5	59.2	59.9	a	a	a	a
7 ^b	8.2	45	99.2	42.3	42.9	0 ^c	3.4	24.0	27.4
8 ^b	8.2	60	99.3	0 ^d	0 ^d	a	a	a	a

^a Not measured (see Table S3).

^b V_{METSO} = 0.7 mL.

^c See footnote [2] in the main text and Table S3 (entry 8).

^d See footnote [1] in the main text and Table S3 (entry 9).

270

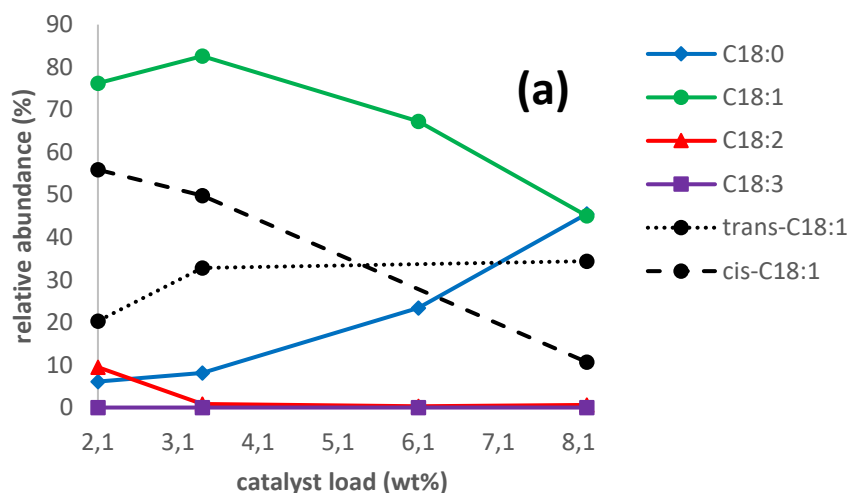
271 4. Discussion

272 *n*-Heptane was selected as reaction medium of the hydrogenation process because of low
 273 viscosity (see later on) and notorious poor tendency of this solvent to compete with the reactants for
 274 the active sites at the catalyst surface [47].⁵ In the hydrocarbon solvent the mixtures A and B can be
 275 effectively converted into C18:1 monoenes over Pd/C under mild conditions of temperature (15 °C)
 276 and H₂ pressure (0.1 MPa). FAME mixture A was hydrogenated to C18:1 with yield and selectivity
 277 respectively of 91.3% and 94.1% within an acceptable time of 60 min (entry 6, Table 1).
 278 Remarkably, despite the almost quantitative conversion of the diene component (97.0%), stearate
 279 abundance did not exceed 5.5% in the final mixture (entry 7, Table S1), while the percentage of *E*-
 280 C18:1 isomers⁶ and C=C bond scrambling⁴ in the C18:1 product were respectively 39.6 and 24%.⁷

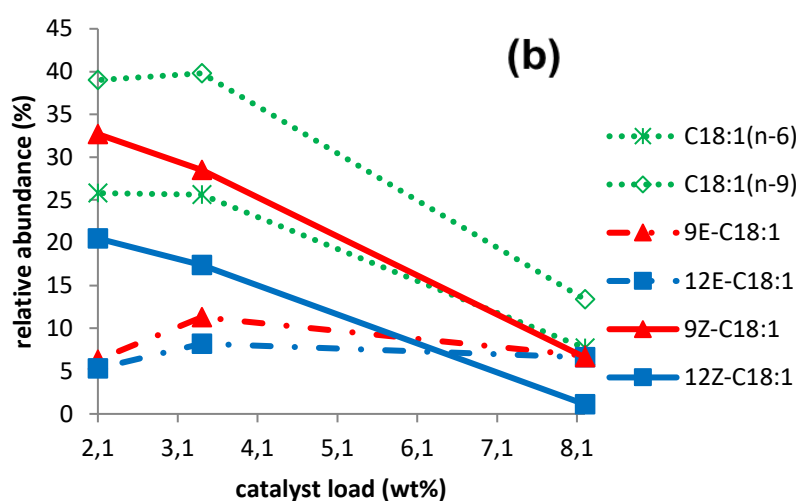
⁵ Elsewhere [45] we have shown that partial hydrogenation of a C18:3-rich FAME mixture proceeded faster and more selectively towards C18:1 in *n*-heptane than in solventless conditions or in donor solvents, such as MeOH, THF, dimethyl carbonate.

⁶ [(%)*E*-C18:1/(%)C18:1]×100

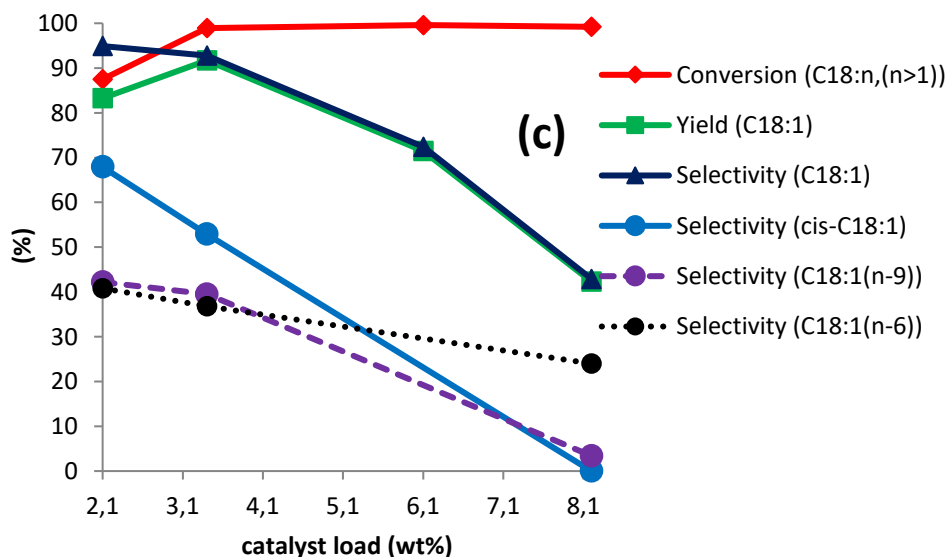
⁷ We probed the recyclability of the catalyst (Fig. S6). The catalyst was recovered quantitatively by filtration, dried and reused several times (experimental conditions: 15 °C, 0.1 MPa of H₂, 1 h; cat. load: 5.7 wt% (150 mg); FAME mixture A: 3.0 mL; *n*-heptane (15 mL)). A diminution of activity was observed after the second cycle, as demonstrated by the decrease of both C_{C18:2} and Y_{C18:1} (from 98% and 91% to 41% and 39%, respectively). After the third cycle, C_{C18:2} and Y_{C18:1} decreased more slowly and were, respectively, equal to 22% and 19 % after 6 cycles. S_{C18:1} did not change significantly after each cycle (93-95%).



281



282



283

284 **Fig. 2.** Partial hydrogenation (0.1 MPa H₂, 15 °C, 45 min) of METSO mixture B (1 mL) over Pd/C
 285 in *n*-heptane (5 mL): influence of catalyst load. When using a catalyst load of 8.2 wt%, *cis*-C18:1
 286 abundance in the hydrogenated mixture was found to be lower than the initial value (Entry 8, Table
 287 S3), so $S_{cis-C18:1}$ has been placed equal to 0.²
 288

289 Satisfactory C18:1 yield and selectivity (respectively 67.7% and 85.6% (entry 5, Table 2) or 73.5%
290 and 74.1% (entry 3, Table 2)) were also achieved under moderate H₂ pressure (1 MPa) at the very
291 mild temperature of 0°C, using a lower catalyst load (1.0 or 2.1 wt%, respectively): with a loading
292 as low as 1.0 wt% both formation of *E*-monoenes ($[(\%)E\text{-C18:1}/(\%)C18:1]\times 100 = 12.5\%$) and C=C
293 scrambling (7%) were quite contained after 45 min (entry 5, Table 2; entry 5, Table S2), despite
294 the advanced state of conversion (79.7%). Overall, these results stand very well the comparison
295 with those available in the literature for the hydrogenation of FAME mixtures of comparable
296 composition in presence of more complex catalytic systems, active under higher pressures and/or at
297 more elevated temperatures (Table S6). Analogously, at 15°C and 0.1 MPa H₂, METSO mixture B
298 was hydrogenated to C18:1 monoenes in a short time (45 min) with yield and selectivity of 83.3%
299 and 94.9% or 91.7% and 92.8%, depending on the used catalyst load (see, respectively, entries 1
300 and 2 in Table 3). The C18:2 component was drastically curtailed at the end of the catalytic run
301 (entries 2 and 3, Table S3). When using a catalyst load of 2.1 wt%, the percentages of *trans*-
302 monoenes⁶ and C=C bond scattering⁴ in the final product were respectively 26.6 and 15.0%, while
303 stearate abundance was still very modest (6.1%; entry 2, Table S3). These data compare well with
304 those obtained by hydrogenating FAME mixtures of analogous composition over Cu-based
305 catalysts (Table S7), well known for the very high selectivity in reducing polyenes to monoenes, but
306 active at higher temperatures and pressures [35-37].

307 Table 4 compares a few parameters, such as cold filter plugging point (CFPP), pour point
308 (PP), cloud point (CP), iodine value (IV), oxidation stability (OS) and cetane number (CN), for the
309 starting mixtures A and B and the relevant upgraded FAMES (H-FAME A and H-METSO)
310 obtained by partial hydrogenation under the above conditions. CFPP, PP, CP, IV, OS, CN are
311 important parameters to define quality and properties of biodiesel. Remarkably, the hydrogenated
312 mixtures displays markedly improved values of IV, OS and CN, that fall within the limits fixed by
313 European laws (UNI EN 14214: $IV \leq 120 \text{ g}_{I_2}/100\text{g}$; $OS \geq 6.0 \text{ h}$; $CN \geq 51$), and still acceptable
314 values for the cold flow properties (CFPP, CP, PP). As a whole, the above findings deserve

Table 4
 Predicted values of CFPP, CP, PP, IV, OS and CN for the starting FAMES (mixture A and METSO mixture B) and upgraded biodiesels (H-FAME A and H-METSO) obtained by partial hydrogenation.^a

FAME mixture	Experimental conditions	CFPP (°C)	CP (°C)	PP (°C)	IV (g ₁₂ /100g)	OS (h)	CN
FAME A		-12.4	-2.7	-9.8	145.6	4.3	40.8
H-FAME A	See Entry 6, Table 1	-6.4	-2.8	-9.8	82.9	61.8	34.9
H-FAME A	See Entry 5, Table 2	-0.3	-2.7	-9.8	90	11.2	53.4
METSO		-9.8	-1.1	-8.0	151.3	4.1	39.4
H-METSO	See Entry 1, Table 3	-4.4	-1.1	-7.8	86.3	15.0	54.1

^a Values calculated by using BiodieselAnalyzer© Software [48]

322

323 attention, being relevant to formulation of 2nd-generation biodiesel from alternative C18:2-rich oils
 324 derived from renewable resources that do not compete with food production.

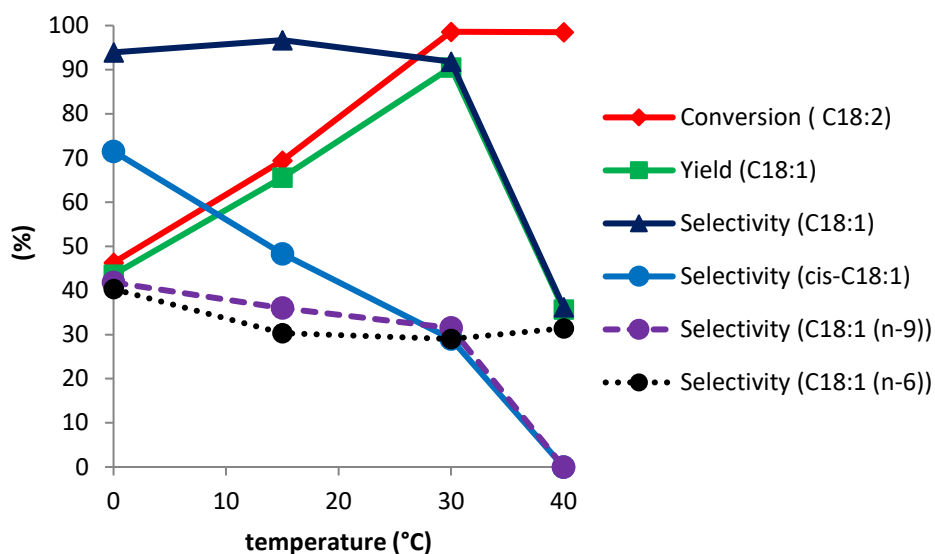
325 Fig. S1a clearly shows that the hydrogenation reaction proceeds through consecutive
 326 reactions C18:2→C18:1→C18:0. In the first phases of the process the hydrogenation mainly
 327 involves linoleate. This species is not significantly implicated in *cis/trans* isomerization side-
 328 processes. In fact, no significant increase or accumulation of geometric isomers of the starting
 329 Z9,Z12-C18:2 diene can be observed (Table S1). The conversion of the C18:2 FAMES (mostly
 330 linoleate) results in the transitory accumulation of the C18:1 component that, after reaching a
 331 maximum, decreases because of C18:1→C18:0 hydrogenation. Notably, methyl stearate begins to
 332 rise more rapidly when most of diene component (~70%) has reacted, showing that the diene
 333 component reacts with H₂ faster than C18:1 monoenes.⁸ Nevertheless, in *n*-heptane, Pd/C can
 334 effectively promote also the full hydrogenation of the FAME mixtures B and A up to the C18:0
 335 stage (93-100% yield) under uncommon very mild conditions (entry 9, Table S3; entry 12, Table
 336 S1). The latter results are worthwhile as methyl stearate is an industrially relevant product that finds
 337 application in several fields (detergents, emulsifiers, wetting agents, stabilizers, resins, lubricants,
 338 plasticizers). Full hydrogenation of C18:m (m = 1,2) FAME mixtures to stearate has been recently

⁸ This can be ascribed to the fact that (i) polyenes are adsorbed on catalyst surface more strongly than monoenes [37] and (ii) polyenes with double bonds separated by a single CH₂-unit react more rapidly than monoenes (or polyenes with double bonds separated by several CH₂-units) [49].

339 achieved by using water soluble Rh-complexes as catalysts, at higher temperatures (80-90 °C; 30-
340 60 min) and under H₂ pressure (4-6 MPa) [25].

341 The *cis*-C18:1 component first grows with time (Fig. S1a), reaches a maximum and then
342 decreases because of *cis*-C18:1 → C18:0 hydrogenation and *cis* → *trans* isomerization side-processes.
343 Accordingly, the decrease of the *cis*-C18:1 monoenes is accompanied by the increase both of
344 stearate and the *trans*-C18:1 component. The incidence of the latter side-processes is, at the
345 beginning ($t \leq 60$ min), quite limited, but it becomes more and more weighty with time. The *E*-
346 C18:1 component, after an initial increase, displays a peak and then decreases with time because of
347 *trans*-C18:1 → C18:0 hydrogenation. The temporary accumulation of *trans*-C18:1 monoenes at
348 expenses of the *cis*-C18:1 isomers supports that (i) *cis*-C18:1 → *trans*-C18:1 isomerization takes
349 place faster than conversion of the *trans*-C18:1 component to stearate, and (ii) in the final phases
350 C18:1 full hydrogenation to stearate involves mainly the *trans*-C18:1 component. Analogous trends
351 are evident also when working under H₂ pressure (Fig. S4a). Noteworthily, at atmospheric pressure
352 (0.1 MPa H₂; Fig. S1a), the *trans*-C18:1 component increases initially ($t \leq 60$ min) more rapidly
353 than stearate, differently from what happens under H₂ pressure (Fig. S4a) wherein, initially ($t \leq 45$
354 min), the curve of formation of stearate rises faster and almost overlaps with that of *trans*-C18:1
355 monoenes. This agrees with the fact that the higher H₂ pressure, by increasing H₂ availability at the
356 catalyst surface, tends to favor C18:1 → C18:0 hydrogenation relative to a side-process that does not
357 consume H₂, such as *cis* → *trans* isomerization.

358 The relative incidence of the above considered side-processes (*cis* → *trans* isomerization and
359 *cis*-C18:1 → C18:0 hydrogenation, on the one hand; *trans*-C18:1 → C18:0 hydrogenation, on the
360 other hand) affects $S_{cis-C18:1}$ that decreases over time with the progress of C18:2 conversion (Figs.
361 S1c and S4c). The diminution of $S_{cis-C18:1}$ with conversion becomes more significant when most of
362 C18:2 has reacted (compare Figs. S1a and S1c or, also, Figs. S4a and S4c). This explains the
363 pronounced diminution of $S_{cis-C18:1}$ under those conditions that promote faster conversion of
364 polyene, such as, for instance, higher catalyst load (Fig. 2c) or temperature (Fig. 3). Table 1



365

366 **Fig. 3.** Partial hydrogenation (0.1 MPa H₂, 30 min) of FAME mixture A (1 mL) over Pd/C (catalyst
 367 load: 5.7 wt%) in *n*-heptane (5 mL) at different temperatures. $S_{cis-C18:1}$ and $S_{C18:1(n-9)}$ at 40 °C
 368 were placed equal to 0 as the abundances of the relevant components (*cis*-C18:1 and C18:1(n-9),
 369 respectively) in the hydrogenated mixture were lower than the initial values.²

370

371 (compare entries 5 and 2 or, also, entries 6 and 3) allows to highlight the effect of temperature on
 372 $S_{cis-C18:1}$, at comparable values of C18:2 conversion: $S_{cis-C18:1}$ diminishes with the increase of
 373 temperature, suggesting that the higher the temperature the greater the weight of the above side-
 374 processes relative to C18:2→C18:1 conversion.

375 The abundances of the C18:1(n-9) and C18:1(n-6) regioisomers grow at comparable rate in
 376 the initial phases of the process (Figs. S1b and S4b). This accounts for the initially very close values
 377 of $S_{C18:1(n-9)}$ and $S_{C18:1(n-6)}$. Both the components reach a maximum when most of diene component
 378 has reacted and stearate formation is still modest (Figs. S1a and S4a), and then begin decreasing
 379 because of larger occurrence of C18:1 hydrogenation to stearate and double bond migration. The
 380 faster diminution of C18:1(n-9) monoenes may reflect differences in the hydrogenation and/or
 381 migration rate of the double bond in 9-position relative to that in 12-position, also in virtue of the
 382 higher concentration of the C18:1(n-9) component (due to the presence of oleate in the starting
 383 mixtures). Consequently, $S_{C18:1(n-9)}$ may differ appreciably from $S_{C18:1(n-6)}$ for longer reaction times
 384 (Figs. S1c and S4c). The extent of C=C scrambling⁴ becomes particularly important when polyenes

385 have been reduced to monoenes (see, for instance, entries 2-5 in Table S1 or entries 4-6 in Table
 386 S2). C=C scrambling is favored by higher temperature,⁹ and it is more moderate with lower catalyst
 387 loadings.¹⁰ Tables S1- S4 allow to compare the extent of C=C scattering in the *cis*- and *trans*-C18:1
 388 components:¹¹ C=C scattering in the *cis*-C18:1 component is not so large as for the *trans*-C18:1
 389 monoenes, but it increases over reaction time (Tables S1 and S2), with temperature (Table S1;
 390 entries 2, 6, 9, 11 or 3, 7, 10), the catalyst load (entries 2 and 4, Table S2; entries 2, 3 and 8, Table
 391 S3).

392 Partial hydrogenation of FAME mixture A was investigated also under solvent-free
 393 conditions (0 °C, 1 MPa; Tables S4 and S5). In absence of solvent the hydrogenation reaction
 394 proceeded more slowly than in *n*-C₇H₁₆ (Entries 1 and 2, Table S5); besides, under solventless
 395 conditions, despite the lower C18:2 conversion, $S_{cis-C18:1}$ and the sum $S_{C18:1(n-9)}+S_{C18:1(n-6)}$ were less
 396 attractive suggesting that the formation of geometric and positional isomers is more favored than in
 397 *n*-heptane. The latter features may be related with the lower availability of H₂ at the catalyst surface
 398 under solvent-free conditions because of (i) the higher viscosity of the reaction medium¹² and (ii)
 399 the higher concentration of substrate (FAMES) that can compete more effectively than H₂ for the
 400 active sites on catalyst surface. This slows down not only the conversion C18:2→C18:1 but also the
 401 C18:1→C18:0 step,¹³ and enhances the incidence of those reactions, such as geometric and
 402 positional isomerization, that do not consume H₂ [3].

403

404

⁹ In Table 1 compare the values of $S_{C18:1(n-9)}+S_{C18:1(n-6)}$, calculated at comparable polyene conversions, at 0 °C (75.9%; entry 5) and 15 °C (66.3%; entry 2) or at 15 °C (66.4%; entry 6) and 30 °C (60.4%; entry 3).

¹⁰ In Table 3 compare the higher value of $S_{C18:1(n-9)}+S_{C18:1(n-6)}$ in entry 1 (83%; catalyst load: 2.1 wt%) with the lower one in entry 4 (65.3%; catalyst load: 5.7 wt%), despite the longer reaction time (45 min vs 30 min, respectively) and the higher C18:m conversion (87.5% vs 75.8%, respectively).

¹¹ Double bond scattering in the *cis*- and *trans*-C18:1 components can be estimated, respectively, as follows:

$[(\%)Z-C18:1(\text{total}) - (\%)Z-C18:1(n-9) - (\%)Z-C18:1(n-6)] \times 100 / (\%)Z-C18:1(\text{total});$

$[(\%)E-C18:1(\text{total}) - (\%)E-C18:1(n-9) - (\%)E-C18:1(n-6)] \times 100 / (\%)E-C18:1(\text{total}).$

¹² At 20 °C, for instance, the dynamic viscosity of *n*-heptane is 0.415 mPa×s [50], markedly lower than that of methyl linoleate and methyl oleate at the same temperature (respectively, 4.4844 and 6.4499 mPa×s) [51,52].

¹³ Compare stearate abundance in entry 2, Table S4 (4.5%, after 60 min), and in entry 4, Table S2 (7.8%, after 30 min).

405 5. Conclusions

406 A few representative C18:2 rich (≥ 67 mol%) FAMES, including a FAME mixture obtained
407 from tobacco seed oil, have been selectively (93-95%) converted to C18:1 monoenes with high
408 yield (83-92%), in *n*-heptane, over a Pd(5%)/C catalyst (2.1-5.7 wt%), under very mild conditions
409 (15 °C, 0.1 MPa, 45-60 min). Remarkably, despite the advanced conversion of the C18:2
410 component, stearate formation was kept within tolerable limits (5.5-8.1%), while *E*-C18:1
411 formation and C=C bond scattering among the C18:1 monoenes were respectively as low as 20.3-
412 34.8% and 15-24%, depending on the FAME mixture used and the working conditions. At 0°C,
413 under moderate pressure of H₂ (1 MPa), *trans*-C18:1 formation and C=C scrambling were less
414 pronounced and respectively equal to 9.0% and 7% after 45 min, using a lower catalyst load (1.0
415 wt%): under the latter conditions, C18:2 content was heavily cut down (from 66.9 to 13.6%), while
416 stearate level in the final mixture was still acceptable (9.3%). These findings compare well with
417 those reported in the literature for the hydrogenation of FAME mixtures of analogous composition
418 with other catalytic systems, less simple and active under not so mild conditions of temperature
419 and/or pressure, and are a step forward towards formulation of 2nd-generation biodiesel from
420 alternative renewable resources that do not interfere with food chain.

421 High C18:1 yield and selectivity required an accurate control of reaction time and
422 temperature because of tendency of the reacting system to convert into stearate through consecutive
423 reactions C18:2→C18:1→C18:0. Notably, in *n*-heptane, Pd/C can act as a versatile catalyst being
424 also able to effectively promote the full hydrogenation of the C18:*m* (*m* = 1-3) components to
425 stearate under uncommon very mild conditions. Also S_{cis-C18:1}, S_{C18:1(n-9)} and S_{C18:1(n-6)} are affected
426 by the reaction conditions. S_{cis-C18:1} decreases over time with the progress of diene conversion, with
427 increasing temperature and catalyst load. C=C scattering in the C18:1 component increases with
428 time, is favored by higher temperature and catalyst load and was found to be more severe among *E*-
429 C18:1 monoenes. Solventless conditions slowed down conversion. In absence of solvent the

430 incidence of the isomerization side-processes affecting the C18:1 component was larger than in the
431 hydrocarbon solvent.

432 **Declaration of competing interest**

433 The authors declare that they have no known competing financial interests or personal
434 relationships that could have appeared to influence the work reported in this paper.

435 **CRedit authorship contribution statement**

436 **Eugenio Quaranta:** Conceptualization, Methodology, Supervision, Writing - review &
437 editing. **Angela Dibenedetto:** Investigation (TSO extraction). **Antonella Colucci:** Investigation
438 (TSO Extraction). **Daniele Cornacchia:** Investigation, Writing - original draft, Validation.

439 **Acknowledgements**

440 This work was financially supported by MIUR, Project “MIUR-PON ENERBIOCHEM
441 PON01_01966”. A.D. thanks Dr. Guendalina Giannuzzi for experimental assistance.

442 **Appendix A. Supplementary Material**

443 Supplementary material related to this article is available as a separate file.

444

445 **References**

- 446 [1] Weidong Z, Jiangwei Y, Xiaoyin Z, Xiaolong Q. Review on the progress of the first-
447 generation biodiesel hydrogenation and upgrading. *Energy Sources A: Recovery Util*
448 *Environ Eff* 2020; 42(21):2704-14. <https://doi.org/10.1080/15567036.2019.1618>.
- 449 [2] Adu-Mensah D, Mei D, Zuo L, Zhang Q, Wang J. A review on partial hydrogenation of
450 biodiesel and its influence on fuel properties. *Fuel* 2019; 251:660-8 and references
451 therein. <https://doi.org/10.1016/j.fuel.2019.04.036>.
- 452 [3] Hu C, Creaser D, Siahrostami S, Grönbeck H, Ojagh H, Skoglundh M. Catalytic
453 hydrogenation of C=C and C=O in unsaturated fatty acid methyl esters. *Catal Sci Technol*
454 2014; 4:2427-44 and references therein. <https://doi.org/10.1039/C4CY00267A>.
- 455 [4] Amin A. Review of diesel production from renewable resources: catalysis, process
456 kinetics and technologies. *Ain Shams Eng J* 2019; 10:821-39 and references therein.
457 <https://doi.org/10.1016/j.asej.2019.08.001>.
- 458 [5] Razon LF. Alternative crops for biodiesel feedstock. *CAB Rev: Perspectives in*
459 *Agriculture, Veterinary Science, Nutrition and Natural Resources* 2009; 4:056.
460 <https://doi.org/10.1079/PAVSNR20094056>.
- 461 [6] Balat M. Potential alternatives to edible oils for biodiesel production - A review of
462 current work. *Energy Convers Manage* 2011; 52:1479-92.
463 <https://doi.org/10.1016/j.enconman.2010.10.011>.
- 464 [7] Ramos M, Dias APS, Puna JF, Gomes J, Bordado JC. Review on biodiesel production
465 processes and sustainable raw materials. *Energies* 2019; 12: 4408.
466 <https://doi.org/10.3390/en12234408>.
- 467 [8] Studentschnig AFH, Schober S, Mittelbach M. Partial Hydrogenation of Fish Oil Methyl
468 Esters for the Production of Biofuels. *Energy Fuel* 2015; 29(6): 3776-3779.
469 <https://doi.org/10.1021/acs.energyfuels.5b00731>.

- 470 [9] Catarino M, Ferreira E, Dias APS, Gomes J. Dry washing biodiesel purification using
471 fumed silica sorbent. Chem Eng J 2020; 386:123930.
472 <https://doi.org/10.1016/j.cej.2019.123930>.
- 473 [10] Numwong N, Luengnaruemitchai A, Chollacoop N, Yoshimura Y. Effect of metal type
474 on partial hydrogenation of rapeseed oil-derived FAME. J Am Oil Chem Soc 2013;
475 90:1431-38 and references therein. <https://doi.org/10.1007/s11746-013-2276-2>.
- 476 [11] Ravasio N, Zaccheria F, Gargano M, Recchia S, Fusi A, Poli N, Psaro R.
477 Environmentally friendly lubricants through selective hydrogenation of rapeseed oil over
478 supported copper catalysts. Appl Catal A 2002; 233:1-6. [https://doi.org/10.1016/S0926-](https://doi.org/10.1016/S0926-860X(02)00128-X)
479 [860X\(02\)00128-X](https://doi.org/10.1016/S0926-860X(02)00128-X).
- 480 [12] Hongmanorom P, Luengnaruemitchai A, Chollacoop N, Yoshimura N. Effect of the
481 Pd/MCM-41 pore size on the catalytic activity and *cis-trans* selectivity for partial
482 hydrogenation of canola biodiesel. Energy & Fuels 2017; 31:8202-9.
483 <https://doi.org/10.1021/acs.energyfuels.7b00832>.
- 484 [13] Rungsi AN, Truong TH, Thunyaratchatanon C, Luengnaruemitchai A, Chollacoop N,
485 Chen S-Y, Mochizuki T, Takagi H, Yoshimura Y. Tuning the porosity of sulfur-resistant
486 Pd-Pt/MCM-41 bimetallic catalysts for partial hydrogenation of soybean oil-derived
487 biodiesel. Fuel 2021; 298:120658. <https://doi.org/10.1016/j.fuel.2021.120658>.
- 488 [14] Carvalho MS, Lacerda RA, Leão JPB, Scholten JD, Neto BAD, Suarez PAZ. In situ
489 generated palladium nanoparticles in imidazolium-based ionic liquids: a versatile medium
490 for an efficient and selective partial biodiesel hydrogenation. Catal Sci Technol 2011;
491 1:480-8. <https://doi.org/10.1039/c0cy00028k>.
- 492 [15] Mochizuki T, Abe Y, Chen S-Y, Toba M, Yoshimura Y. Oxygen-assisted hydrogenation
493 of Jatropha oil-derived biodiesel fuel over alumina-supported Pd catalyst to produce
494 hydrotreated fatty acid methyl esters for high-blends fuels. ChemCatChem 2017; 9:2633-
495 7. <https://doi.org/10.1002/cctc.201700071>.

- 496 [16] Phumpradit S, Reubroycharoen P, Kuchonthara P, Ngamcharussrivichai C, Hinchiranan
497 N. Partial hydrogenation of palm oil-derived biodiesel over Ni/electrospun silica fiber
498 catalysts. *Catalysts* 2020; 10(9):993. <https://doi.org/10.3390/catal10090993>.
- 499 [17] Erenturk S, Korkut O. Effectiveness of activated mistalea (*Viscum album* L.) as a
500 heterogeneous catalyst for biodiesel partial hydrogenation. *Renew Energy* 2018; 117:374-
501 9. <https://doi.org/10.1016/j.renene.2017.10.092>.
- 502 [18] Thunyaratchatanon C, Luengnaruemitchai A, Chollacoop N, Yoshimura Y. Catalytic
503 upgrading of soybean oil methyl esters by partial hydrogenation using Pd catalysts. *Fuel*
504 2016; 163:8-16. <https://dx.doi.org/10.1016/j.fuel.2015.09.026>.
- 505 [19] Thunyaratchatanon C, Luengnaruemitchai A, Chollacoop N, Chen S-Y, Yoshimura Y.
506 Catalytic hydrogenation of soybean oil-derived fatty acid methyl esters over Pd supported
507 on Zr-SBA-15 with various Zr loading levels for enhanced oxidative stability. *Fuel*
508 *Process Technol* 2018; 179:422-35. <https://doi.org/10.1016/j.fuproc.2018.07.014>.
- 509 [20] Rungsi AN, Luengnaruemitchai A, Chollacoop N, Chen S-Y, Mochizuki T, Takagi H,
510 Yoshimura Y. Preparation of MCM-41-supported Pd–Pt catalysts with enhanced activity
511 and sulfur resistance for partial hydrogenation of soybean oil-derived biodiesel fuel. *Appl*
512 *Catal A* 2020; 590:117351. <https://doi.org/10.1016/j.apcata.2019.117351>
- 513 [21] Chen S-Y, Chang A, Rungsi AN, Attanatho L., Chang C-L, Pan J-H, Suemanotham A,
514 Mochizuki T, Takagi H, Yang C-M, Luengnaruemitchai A, Chou H-H. Superficial Pd
515 nanoparticles supported on carbonaceous SBA-15 as efficient hydrotreating catalyst for
516 upgrading biodiesel fuel. *Appl Catal A* 2020; 602:117707.
517 <https://doi.org/10.1016/j.apcata.2019.117707>.
- 518 [22] S.-Y. Chen, L. Attanatho, T. Mochizuki, Q. Zheng, M. Toba, Y. Yoshimura, P.
519 Somwongsa, S. Lao-Ubol, Influences of the Support Property and Pd Loading on
520 Activity of Mesoporous Silica-Supported Pd Catalysts in Partial Hydrogenation of Palm

- 521 Biodiesel Fuel, *Adv. Porous Mater.* 4 (2016) 230-237.
522 <https://doi.org/10.1166/apm.2016.1116>
- 523 [23] Numwong N, Luengnaruemitchai A, Chollacoop N, Yoshimura Y. Partial hydrogenation
524 of polyunsaturated fatty acid methyl esters over Pd/activated carbon: effect of type of
525 reactor. *Chem Eng J* 2012 210:173-181. <https://dx.doi.org/10.1016/j.cej.2012.08.034>.
- 526 [24] Papadopoulos CE, Lazaridou A, Koutsoumba A, Kokkinos N, Christoforidis A, Nikolaou
527 N. Optimization of cotton seed biodiesel quality (critical properties) through
528 modification of its FAME composition by highly selective homogeneous hydrogenation.
529 *Bioresour Technol* 2010; 101:1812-9. <https://doi.org/10.1016/j.biortech.2009.10.016>.
- 530 [25] Kaika N, Panopoulou C, Anagnostopoulou E, Fakas C, Lilas P, Stavroulaki D,
531 Papadogianakis G. Novel full hydrogenation reaction of methyl esters of palm kernel and
532 sunflower oils into methyl stearate catalyzed by rhodium, ruthenium and nickel
533 complexes of bidentate hexasulfonated o-phenylendiphosphite ligands. *Catal Lett* 2019;
534 149:580-90. <https://doi.org/10.1007/s10562-018-2642-7>.
- 535 [26] Vasiliou C, Bouriazos A, Tsihla A, Papadogianakis G. Production of hydrogenated
536 methyl esters of palm kernel and sunflower oils by employing rhodium and ruthenium
537 catalytic complexes of hydrolysis stable monodentate sulfonated triphenylphosphite
538 ligands. *Appl Catal B* 2014;158-159:373-81.
539 <https://doi.org/10.1016/j.apcatb.2014.04.046>.
- 540 [27] Bouriazos A, Vasiliou C, Tsihia A, Papadogianakis G. Catalytic conversions in green
541 aqueous media. Part 8: Partial and full hydrogenation of renewable methyl esters of
542 vegetable oils. *Catal Today* 2014;247:20-32. <https://doi.org/10.1016/j.cattod.2014.08.021>.
- 543 [28] Bouriazos A, Sotiriou S, Vangelis C, Papadogianakis G. Catalytic conversions in green
544 aqueous media: Part 4. Selective hydrogenation of polyunsaturated methyl esters of
545 vegetable oils for upgrading biodiesel. *J Organomet Chem* 2010; 695:327-37.
546 <https://doi.org/10.1016/j.jorganchem.2009.10.045>.

- 547 [29] Nikolaou N, Papadopoulos CE, Lazaridou A, Koutsoumba A, Bouriazos A,
548 Papadogianakis G. Partial hydrogenation of methyl esters of sunflower oil catalyzed by
549 highly active rhodium sulfonated triphenylphosphite complexes. *Catal Commun* 2009;
550 10:451-5. <https://doi.org/10.1016/j.catcom.2008.10.026>.
- 551 [30] Liu W, Xu L, Lu G, Zhang H. Selective partial hydrogenation of methyl linoleate using
552 highly active palladium nanoparticles in polyethylene glycol. *ACS Sustainable Chem Eng*
553 2017; 5:1368-75. <https://doi.org/10.1021/acssuschemeng.6b01823>.
- 554 [31] Souza BS, Pinho DMM, Leopoldino EC, Suarez PAZ, Nome F. Selective partial
555 biodiesel hydrogenation using highly active supported palladium nanoparticles in
556 imidazolium-based ionic liquid. *Appl Catal A* 2012; 433-434:109-14.
557 <https://doi.org/10.1016/j.apcata.2012.05.006>.
- 558 [32] Pérez-Cadenas AF, Kapteijn F, Zieverink MMP, Moulijn JA. Selective hydrogenation of
559 fatty acid methyl esters over palladium on carbon-based monoliths: structural control of
560 activity and selectivity. *Catal Today* 2007; 128:13-7.
561 <https://doi.org/10.1016/j.cattod.2007.05.006>.
- 562 [33] Pérez-Cadenas AF, Zieverink MMP, Kapteijn F, Moulijn JA. Selective hydrogenation of
563 fatty acid methyl esters on palladium catalysts supported on carbon-coated monoliths.
564 *Carbon* 2006; 44:173-6. <https://doi.org/10.1016/j.carbon.2005.08.014>.
- 565 [34] Pérez-Cadenas AF, Zieverink MMP, Kapteijn F, Moulijn JA. High performance
566 monolithic catalysts for hydrogenation reactions. *Catal Today* 2005; 105:623-8.
567 <https://doi.org/10.1016/j.cattod.2005.06.017>.
- 568 [35] Zaccheria F, Psaro R, Ravasio N. Selective hydrogenation of alternative oils: a useful tool
569 for the production of biofuels. *Green Chem* 2009; 11:462-5.
570 <https://doi.org/10.1039/B817625F>.

- 571 [36] Zaccheria F, Psaro R, Ravasio N, Bondioli P. Standardization of vegetable oils
572 composition to be used as oleochemistry feedstock through a selective hydrogenation
573 process. *Eur J Lipid Sci Technol* 2012;114:24-30. <https://doi.org/10.1002/ejlt.201100044>.
- 574 [37] Zaccheria F, Ravasio N. Partial reduction of polyenes. In: de Vries JG, editor. *Science of*
575 *Synthesis: Catalytic reduction in organic synthesis 1*, Thieme; 2018, p. 91-125.
576 <https://doi.org/10.1055/sos-SD-226-00049>.
- 577 [38] Banković-Ilčić IB, Stamenković OS, Veljković VB. Biodiesel production from non-edible
578 plant oils. *Renew Sustain Energy Rev* 2012; 16:3621-47.
579 <https://doi.org/10.1016/j.rser.2012.03.002>.
- 580 [39] Atabani AE, Silitonga AS, Ong HC, Mahlia TMI, Masjuki HH, Badruddin IA, Fayaz H.
581 Non-edible vegetable oils: a critical evaluation of oil extraction, fatty acid compositions,
582 biodiesel production, characteristics, engine performance and emissions production.
583 *Renew Sustain Energy Rev* 2013;18:211-45. <http://dx.doi.org/10.1016/j.rser.2012.10.013>.
- 584 [40] Bart JCJ, Palmeri N, Cavallaro S. *Biodiesel science and technology: from soil to oil*.
585 Woodhead Publishing Limited and CRC Press LLC; 2010, Chapter 5.
- 586 [41] Giannelos PN, Zannikos F, Stournas S, Lois E, Anastopoulos G. Tobacco seed oil as an
587 alternative diesel fuel: physical and chemical properties. *Ind Crop Prod* 2002; 16:1-9.
588 [https://doi.org/10.1016/S0926-6690\(02\)00002-X](https://doi.org/10.1016/S0926-6690(02)00002-X).
- 589 [42] García-Martínez N, Andreo-Martínez P, Quesada-Medina J, Pérez de los Ríos A, Chica
590 A, Beneito-Ruiz R, Carratalá-Abril J. Optimization of non-catalytic transesterification of
591 tobacco (*Nicotiana tabacum*) seed oil using supercritical methanol to biodiesel
592 production. *Energy Convers Manage* 2017; 131:99-108.
593 <http://dx.doi.org/10.1016/j.enconman.2016.10.078>.
- 594 [43] Usta N, Aydogan B, Çon AH, Uguzdogan E, Özkal SG. Properties and quality
595 verification of biodiesel produced from tobacco seed oil. *Energy Convers Manage* 2011;
596 52:2031-39. <http://dx.doi.org/10.1016/j.enconman.2016.10.078>.

- 597 [44] Toebes ML, Dillen JAV, de Jong KP. Synthesis of supported palladium catalysts. *J Mol*
598 *Catal A* 2001; 173:75-98. [https://doi.org/10.1016/S1381-1169\(01\)00146-7](https://doi.org/10.1016/S1381-1169(01)00146-7).
- 599 [45] Quaranta E, Cornacchia D. Partial hydrogenation of a C18:3-rich FAME mixture over
600 Pd/C. *Renew Energy* 2020; 157:33-42. <https://doi.org/10.1016/j.renene.2020.04.122>.
- 601 [46] (CEE) N. 2568/91 - Annex II, (CEE) N. 2568/91 - Annex V and EN 14105:2011.
- 602 [47] Augustine RL. *Heterogeneous Catalysis for the Synthetic Chemist*. CRC Press; 1995.
- 603 [48] Talebi AF, Tabatabaei M, Chisti Y. BiodieselAnalyzer@: A user-friendly software for
604 predicting the properties of prospective biodiesel. *Biofuel Res J* 2014; 2: 55–57.
605 <https://dx.doi.org/10.18331/BRJ2015.1.2.4>.
- 606 [49] Santacesaria E, Parrella P, Diserio M, Borrelli G. Role of mass transfer and kinetics in the
607 hydrogenation of rapeseed oil on a supported palladium catalyst. *Appl Catal A* 1994;
608 116:269-94. [https://doi.org/10.1016/0926-860X\(94\)80294-7](https://doi.org/10.1016/0926-860X(94)80294-7).
- 609 [50] Landaverde-Cortes DC, Estrada-Baltazar A, Iglesias-Silva GA, Hall KR. Densities and
610 viscosities of MTBE + heptane or octane at $p = 0.1$ MPa from (273.15 to 363.15) K. *J*
611 *Chem Eng Data* 2007; 52:1226-32. <https://doi.org/10.1021/je600554h>.
- 612 [51] Pratas MJ, Freitas S, Oliveira MB, Monteiro SC, Lima AS, Coutinho JAP. Densities and
613 viscosities of minority fatty acid methyl and ethyl esters present in biodiesel. *J Chem Eng*
614 *Data* 2011; 56:2175-80. <https://doi.org/10.1021/je1012235>.
- 615 [52] Pratas MJ, Freitas S, Oliveira MB, Monteiro SC, Lima AS, Coutinho JAP. Densities and
616 viscosities of fatty acid methyl and ethyl esters. *J Chem Eng Data* 2010; 55:3983-90.
617 <https://doi.org/10.1021/je100042c>.